Stochastic Shilnikov maps

1987 J. Phys. A: Math. Gen. 20 1333

(http://iopscience.iop.org/0305-4470/20/6/017)

J. Phys. A: Math. Gen. **20** (1987) 1333-1343. Printed in the UK

Stochastic Shilnikov maps

J S Satchell† and Sarben Sarkar

Centre for Theoretical Studies, Royal Signals and Radar Establishment, Great Malvern, Worcestershire WR14 3PS, UK

Received 21 February 1986, in final form 24 July 1986

Abstract. Fluctuations in dynamical systems may give rise naturally to stochastic maps which, in the absence of fluctuations, reduce to maps similar to those considered by Shilnikov. Noise appears in a highly non-trivial manner. The effect of the noise on the chaotic dynamics is studied. It is shown that the different noise terms can give rise to radically different behaviour.

1. Introduction

Dynamical systems have recently been much studied numerically [1] and chaotic behaviour has been found. In parallel there has been a great deal of progress in understanding the phenomena in geometrical terms [2]. Particularly influential has been the 'horseshoe' construction of Smale [3] in which a unit square is stretched, bent and contracted into a horseshoe, and the curved part of the horseshoe lies outside the square. The invariant set under such a mapping has a Cantor-like structure both horizontally and vertically. Chaotic attractors possess such invariant sets, which start growing before the actual threshold for chaos. Such horseshoes naturally arise when there are transverse homoclinic orbits [2]. Shilnikov [4] and others [5] have shown this for certain three-dimensional flows. In particular, if there is a homoclinic trajectory to a saddle point with complex eigenvalues where the real eigenvalue has a larger magnitude than the real part of the complex eigenvalues then there are horseshoes present in return maps defined near the homoclinic orbit. Also there is a similar result when the system of three-dimensional differential equations has a Lorenz-type symmetry and the saddle point has real eigenvalues which satisfy $-\lambda_2 > \lambda_1 > -\lambda_3 > 0$. (If the phase space variables are X_1, X_2 and X_3 then the Lorenz symmetry requires the evolution equations to be invariant under $X_1 \to -X_1$, $X_2 \to -X_2$ and $X_3 \to X_3$.) The behaviour of dynamical systems under stochastic perturbations [6, 7] is a growing area of interest, since noise is always present in physical systems. Moreover from general theorems [8] we expect that dissipation in systems is accompanied by fluctuations. In this paper we will construct return maps in the spirit of Shilnikov for some stochastic dynamical systems. Just as the return maps are valuable for the deterministic system in understanding strange invariant sets, we hope that the stochastic versions of these maps will play a role in the understanding of possible noise-induced behaviour. Once we have obtained the maps we will also 'analytically continue' them to parameter regimes outside the scope of the Shilnikov construction. The two types of saddle points

† Also at: Clarendon Laboratory, University of Oxford, UK.

0305-4470/87/061333+11$02.50

mentioned earlier will be primarily considered. A limited amount of work on maps with noise has already been done. The procedure has usually been somewhat *ad hoc*. Typically a simple additive noise term is appended to a standard map such as the logistic map. This is not an unreasonable procedure and both analytic and numerical results have been obtained for exponents describing the scaling of Lyapounov exponents with noise [9]. However, since maps usually emerge in physical systems through the use of Poincaré sections on dynamical systems, and the Shilnikov construction is a rather natural example of one, it seems interesting to use it to obtain stochastic maps, the stochasticity having been introduced directly into the ordinary differential equations defining the dynamical system. The maps that we obtain are very different from the ones usually studied. The noise appears embedded in the maps in a quite unexpected way. If these maps had been written down without explanation they might well have appeared bizarre. However, they are implied by Shilnikov type constructions which appeal to rather general properties of the underlying systems (such as the relative magnitudes of the eigenvalues at the saddle point) and so should not be too special. We will indeed find quite a rich variety of behaviour, some of which encompasses the phenomena found in earlier work [9]. The universality classes of behaviour found in the presence of noise are thus likely to be diverse.

Once we deal with stochastic maps it is necessary to use probabilistic concepts. The attractor will be the support of the probability distribution for the system. We are interested in ensemble or time averages of quantities (since ergodicity is found to hold). Among the more useful quantities are Lyapounov exponents and dimensions [10] and fractal (or clustering) dimensions [11]. In the next section we will describe the two stochastic Shilnikov maps that we will study. In the last section they will be analysed using the quantities mentioned above.

2. The Shilnikov construction

Without loss of generality the saddle point in the dynamical system can be taken to be at the origin. For the usual Shilnikov case the stochastic dynamical system near the saddle point is taken to be

$$\begin{pmatrix} \dot{x} \\ \dot{y} \\ \dot{z} \end{pmatrix} = \begin{pmatrix} \alpha & -\beta & 0 \\ \beta & \alpha & 0 \\ 0 & 0 & \lambda \end{pmatrix} \begin{pmatrix} x \\ y \\ z \end{pmatrix} + \begin{pmatrix} \varepsilon_1 \xi_1 \\ \varepsilon_2 \xi_2 \\ \varepsilon_3 \xi_3 \end{pmatrix} \tag{1}$$

where ξ_i are independent Gaussian white noises

$$\langle \xi_i(t) \xi_j(t') \rangle = \delta_{ij} \delta(t - t') \qquad i, j = 1, 2, 3 \tag{2}$$

and x, y and z are real variables.

Here $\lambda > -\alpha > 0$; ε_i are small noise strengths. We take a small cylinder of radius r_0 around the origin shown in figure 1. The behaviour of the z variable in (1) decouples from that of x and y and is described by $z(t)$ which is an Ornstein-Uhlenbeck process [12]. If the ε_i in (1) were functions of x, y and z with Taylor expansions around the origin, then the dominant contributions would come from the constant terms in the expansions. Higher-order contributions are very small since they depend on polynomials in x, y and z which are small near the origin. The solution for $z(t)$ is

$$z(t) = z(0)\, e^{\lambda t} + \varepsilon_3\, e^{\lambda t} \int_0^t dt'\, e^{-\lambda t'} \xi_3(t'). \tag{3}$$

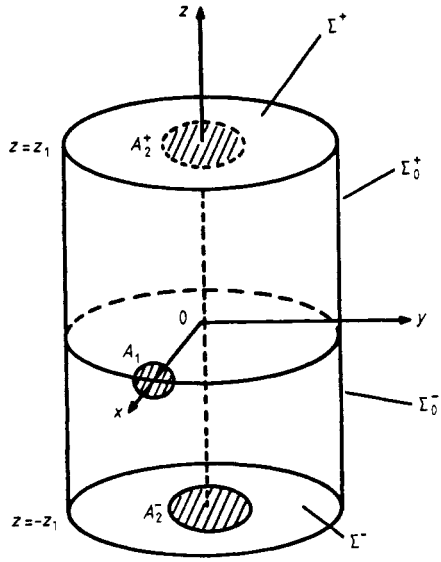

Figure 1. The cylinder used in the Shilnikov construction.

We define

$$\tilde{W}_\lambda(t) = \int_0^t \mathrm{d}t' \, \mathrm{e}^{-\lambda t'} \xi_3(t'). \tag{4}$$

$\tilde{W}_\lambda$ is Gaussian with

$$\langle \tilde{W}_\lambda(t) \rangle = 0 \tag{5}$$

and

$$\langle \tilde{W}_\lambda(t) \, \tilde{W}_\lambda(s) \rangle = \frac{1}{2\lambda} [1 - \theta(t-s) \, \mathrm{e}^{-2\lambda s} - \theta(s-t) \, \mathrm{e}^{-2\lambda t}] \tag{6}$$

with

$$\begin{aligned} \theta(x) &= 1 \qquad x > 0 \\ &= \tfrac{1}{2} \qquad x = 0 \\ &= 0 \qquad x < 0. \end{aligned} \tag{7}$$

If we consider a point initially in A_1 then depending on $z(0)$ and the effect of the random forces it will reach A_2. The time t' at which this happens is given by

$$t' = \frac{1}{\lambda} \log\left(\frac{z_1}{|z(0) + \varepsilon_3 \tilde{W}_\lambda(t')|} \right). \tag{8}$$

Since $z(0)$ and ε_3 are very small we expect $\lambda t'$ to be large almost always and can take

$$\langle (W_\lambda(t'))^2 \rangle \simeq 1/2\lambda. \tag{9}$$

Then we have

$$t' \simeq \frac{1}{\lambda} \log\left(\frac{z_1}{|z(0) + [\varepsilon_3/(2\lambda)^{1/2}]\hat{\xi}_3|} \right) \tag{10}$$

where $\hat{\xi}_3$ is a white noise (with zero mean and unit variance).

It is easy to see that the variables x and y satisfy

$$\dot{x} + \mathrm{i}\dot{y} = (\alpha + \mathrm{i}\beta)(x + \mathrm{i}y) + \varepsilon_1 \xi_1 + \mathrm{i}\varepsilon_2 \xi_2. \tag{11}$$

Consequently

$$x(t) = \mathrm{e}^{\alpha t}(x(0) \cos \beta t - y(0) \sin \beta t) + \int_0^t \mathrm{d}s \exp[\alpha(t-s)][\varepsilon_1 \xi_1(s) \cos \beta(t-s) - \varepsilon_2 \xi_2(s) \sin \beta(t-s)] \tag{12}$$

and

$$y(t) = \mathrm{e}^{\alpha t}(y(0) \cos \beta t + x(0) \sin \beta t) + \int_0^t \exp[\alpha(t-s)][\sin \beta(t-s)\varepsilon_1 \xi_1(s) + \cos \beta(t-s)\varepsilon_2 \xi_2(s)]\, \mathrm{d}s. \tag{13}$$

It can then be shown that

$$x(t') = r_0 \exp\left(\frac{\alpha}{\beta} \hat{\gamma}(z(0)) \right) \cos(\theta + \hat{\gamma}(z(0))) + \varepsilon_1' \hat{\xi}_1 \tag{14}$$

$$y(t') = r_0 \exp\left(\frac{\alpha}{\beta} \hat{\gamma}(z(0)) \right) \sin(\theta + \hat{\gamma}(z(0))) + \varepsilon_2' \hat{\xi}_2 \tag{15}$$

where

$$\hat{\gamma}(t) = \frac{\beta}{\lambda} \log \frac{z_1}{|z + [\varepsilon_3/(2\lambda)^{1/2}]\hat{\xi}_3|} \tag{16}$$

$$\begin{aligned} x(0) &= r_0 \cos \theta \\ y(0) &= r_0 \sin \theta \end{aligned} \tag{17}$$

$\hat{\xi}_1$ and $\hat{\xi}_2$ are independent Gaussian white noises of zero mean and unit variance and ε_1' and ε_2' are constants proportional to ε_1 and ε_2. Equations (14) and (15) define a stochastic map from Σ_0 to $\Sigma^{\pm}$. In order to obtain a return map it is necessary to have a map from $\Sigma^{\pm}$ to Σ_0. This map involves trajectories outside the cylinder where the variables x, y and z are large. Since noise strengths are small it is the deterministic motion which completely dominates there. The map is contracting and we also know that in the absence of noise the point in A_1 with $\theta = 0$ and $z(0) = 0$ is on a homoclinic orbit. The simplest map from $\Sigma^{\pm}$ to Σ_0 which satisfies these requirements is

$$\begin{pmatrix} x \\ y \end{pmatrix} \to \begin{pmatrix} \mu & 0 \\ 0 & \mu \end{pmatrix} \begin{pmatrix} x \\ y \end{pmatrix} \tag{18}$$

with $0 < \mu < 1$. Putting (14), (15) and (18) together we have finally the map

$$\begin{aligned} \theta' &= \mu r_0 \exp(\alpha g) \cos(\theta + \beta g) + \varepsilon_1' \hat{\xi}_1 \\ z' &= \mu r_0 \exp(\alpha g) \sin(\theta + \beta g) + \varepsilon_2' \hat{\xi}_2 \end{aligned} \tag{19}$$

where

$$\lambda g = \log \frac{z_1}{|z + \varepsilon_3' \hat{\xi}_3|}$$

and ε_1', ε_2' and ε_3' are noise strengths. It will turn out to be interesting to study the consequences of this map even when α is non-negative.

We will now turn to the stochastic Lorenz system and proceed very much in the same spirit. Near the origin

$$\begin{pmatrix}\dot{x}\\ \dot{y}\\ \dot{z}\end{pmatrix}=\begin{pmatrix}-\sigma & \sigma & 0\\ r & -1 & 0\\ 0 & 0 & -b\end{pmatrix}\begin{pmatrix}x\\ y\\ z\end{pmatrix}+\begin{pmatrix}\varepsilon_1\hat{\xi}_1\\ \varepsilon_2\hat{\xi}_2\\ \varepsilon_3\hat{\xi}_3\end{pmatrix} \tag{20}$$

and σ, r and b are the standard Lorenz parameters [5, 13]. The eigenvalues λ_1, λ_2 and λ_3 of the matrix in (20) are given by

$$\begin{aligned}\lambda_{\frac{1}{2}}&=\tfrac{1}{2}\{-(1+\sigma)\pm[(1-\sigma)^2+4\sigma r]^{1/2}\}\\ \lambda_3&=-b.\end{aligned} \tag{21}$$

Clearly

$$-\lambda_2>\lambda_1>-\lambda_3>0 \qquad \text{for } r>[1+b(1+\sigma+b)\sigma^{-1}].$$

By defining the variables

$$\alpha_1=\frac{-x(\lambda_2+\sigma)+\sigma y}{\sigma(\lambda_1-\lambda_2)} \tag{22}$$

$$\alpha_2=\frac{x(\lambda_1+\sigma)-\sigma y}{\sigma(\lambda_1-\lambda_2)} \tag{23}$$

we have

$$\begin{pmatrix}\dot{\alpha}_1\\ \dot{\alpha}_2\\ \dot{z}\end{pmatrix}=\begin{pmatrix}\lambda_1 & & \\ & \lambda_2 & \\ & & \lambda_3\end{pmatrix}\begin{pmatrix}\alpha_1\\ \alpha_2\\ z\end{pmatrix}+\begin{pmatrix}\varepsilon_1'\hat{\xi}_1\\ \varepsilon_2'\hat{\xi}_2\\ \varepsilon_3'\hat{\xi}_3\end{pmatrix}. \tag{24}$$

It is convenient in this case to take a box around the origin (as shown in figure 2) rather than a cylinder.

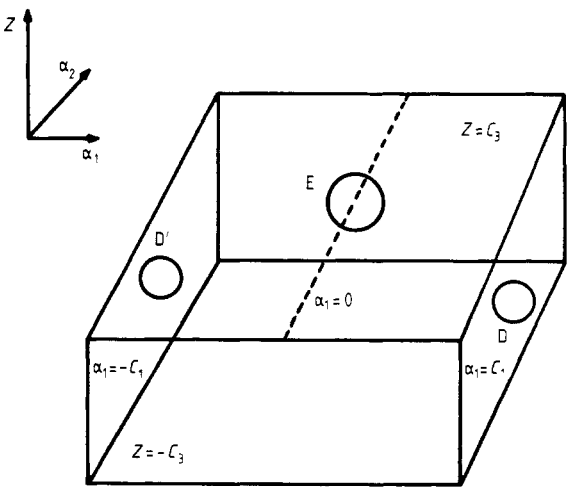

Figure 2. The box used in the Shilnikov construction.

The region E lies in the plane $z = C_3$, D′ in $\alpha_1 = -C_1$ and D in $\alpha_1 = C_1$. The map from E to E can be found using arguments analogous to those given earlier. We will outline the main steps. α_1 satisfies an equation exactly similar to (3), and from this the stochastic time necessary to go from E to D can be found. Hence for the map E → D, D′ we have

$$(\alpha_1, \alpha_2, C_3) \to \left[\operatorname{sgn}(\alpha_1) C_1, \alpha_2 \left(\frac{|\alpha_1| + \varepsilon_1' \xi}{C_1} \right)^{\nu'} + \varepsilon_2' \xi_2, C_3 \left(\frac{|\alpha_1| + \varepsilon_1' \xi_1}{C_1} \right)^{\nu'} - \varepsilon_3' \xi_3 \right] \tag{25}$$

where $\nu' = -\lambda_3/\lambda_1$.

In order to obtain a return map we write the map D → E as

$$(C_1, \alpha_2, z) \to (f_r(\alpha_2, z), g_r(\alpha_2, z), C_3)$$

where f_r and g_r are (differentiable) functions of α_2 and z. Moreover from the Lorenz symmetry the map D′ → E is given by

$$(-C_1, \alpha_2, z) \to (-f_r(-\alpha_2, z), -g_r(-\alpha_2, z), C_3). \tag{26}$$

On composing these maps, the map from E to E is found to have the form

$$\alpha_1 \to \operatorname{sgn}(\alpha_1) \left[A' + B' C_3 \left(\frac{\| \alpha_1 | + \varepsilon_1' \xi_1 |}{C_1} \right)^{\nu'} \right] + \varepsilon_2' \xi_2 \tag{27}$$

with

$$A' = f_r(0, 0)$$

and

$$B' = \partial f_r(0, 0)/\partial z.$$

Just as in the purely deterministic case [5] it is the fact that $(-\lambda_2/\lambda_1) > 1$ and $(-\lambda_3/\lambda_1) < 1$ that allows the stochastic map to be one dimensional. Compared to the stochastic logistic map [9] for a real variable x_n

$$x_{n+1} = \lambda x_n (x_n - 1) + \varepsilon \xi_n \tag{28}$$

(where ξ_n is a Gaussian random variable with zero mean and unit variance) stochastic Shilnikov maps look very unusual. The analytic methods used in previous studies [9] do not apply owing to the multiplicative nature of the noise and also the non-analytic nature of the functions that appear in the maps.

3. The stochastic maps

The (θ, z) map (of (19)) is defined essentially by three parameters α, β and λ but only their ratios are important. We have chosen to fix λ and vary the other two. λ is taken to be 1 and so α is constrained to be between 1 and -1. β can in principle be freely chosen. It is first useful to find the behaviour in the absence of noise.

The attracting sets of the map all seem to lie on a spiral whose pitch depends on β/α. Large values of the ratio give a tightly wound spiral. In the limiting case of $\alpha = 0$ the spiral degenerates into a circle.

For some parameter values we have found more than one attractor, each with its separate basin of attraction. There are, however, some general characteristics. For low β values a fixed point is, in general, found. Larger values of β give chaotic

behaviour. The route to chaos depends on the value of α. We find that the fixed point changes first into a period two limit cycle for $\alpha = 0.2$. As β approaches 1.507 433 793 this limit cycle loses its stability and chaos is reached by the intermittency route. Figure 3(a) shows 200 iterations of the map for $\alpha = 0.2$ and $\beta = 1.51$. The spiral-shaped strange attractor is visible. The nearly stable limit cycle can be seen as a pair of dense accumulation of points.

The situation is different when α is negative. As β is raised the fixed point splits into a two-cycle which then undergoes a period doubling bifurcation sequence to give

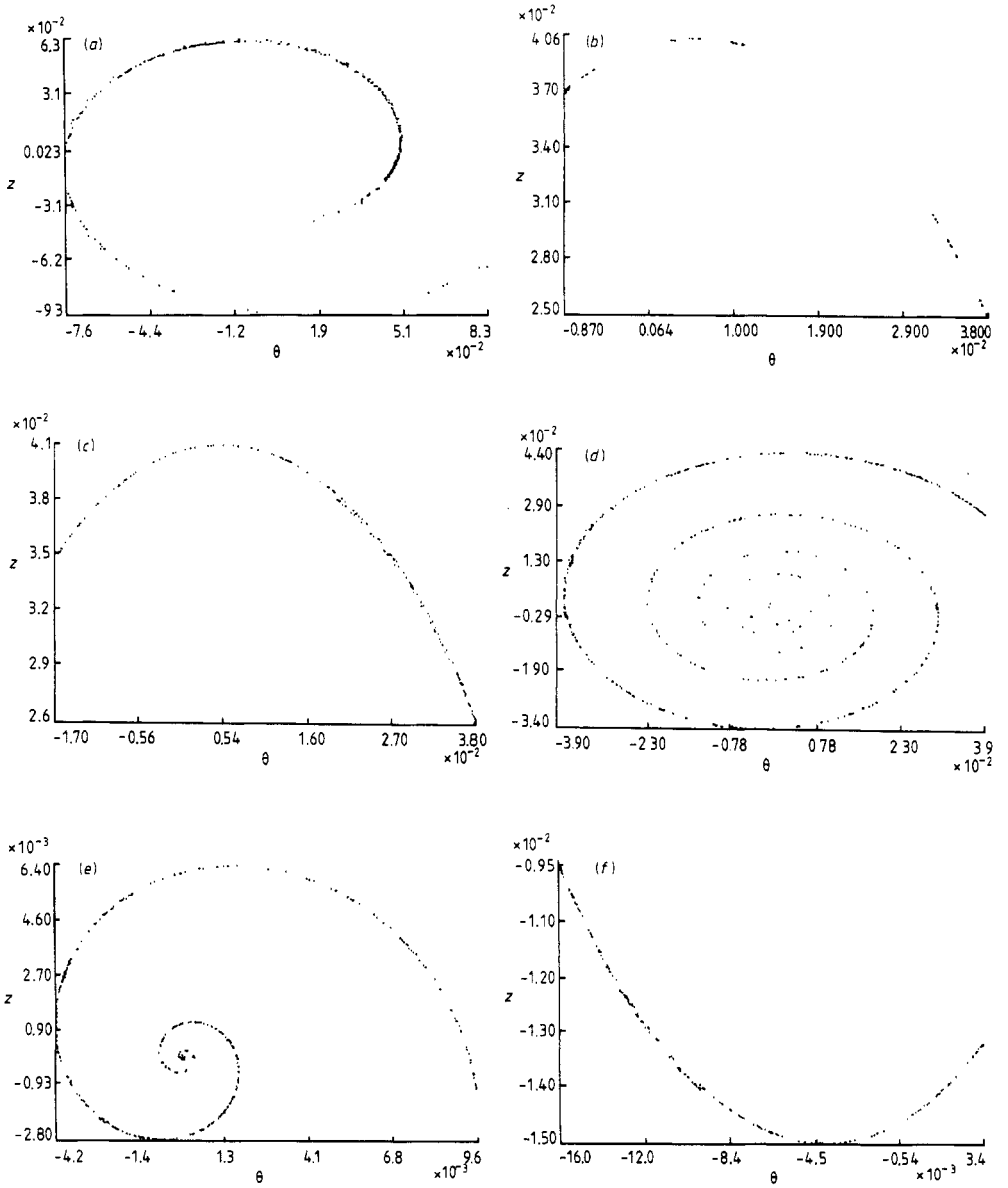

Figure 3. The two-dimensional attractor for (a) $\alpha = 0.2$, $\beta = 1.51$; (b) $\alpha = -0.4$, $\beta = 2.607\,5063$; (c) $\alpha = -0.4$, $\beta = 3.0$; (d) $\alpha = -0.4$, $\beta = 5.0$; (e) $\alpha = -0.8$, $\beta = 3.0$; (f) $\alpha = -0.8$, $\beta = 3.0$.

chaos on a parabolic attractor. Figure 3(b) shows the case of $\alpha = -0.4$ and $\beta = 2.607\,5063$, which is near the accumulation point of the period doubling cascade. If β is raised to 3 the chaos is fully developed and we find the parabolic attractor of figure 3(c), which presumably has further structure which is difficult to see numerically. The parabola splits into two parallel leaves in the right-hand part of the figure. The separation of the leaves increases the higher β is raised above the threshold for chaos. For yet larger β the trajectory moves on a spiral attractor. Figure 3(d) shows 400 iterations for $\beta = 5.0$ and $\alpha = -0.4$.

In general, if β is reduced in small steps, chaotic behaviour on the spiral attractor is found to coexist with other non-chaotic behaviour. At sufficiently low β the attractor is only metastable and trajectories are recaptured by the fixed point. In one case ($\alpha = -0.8$) a third attractor is found. This undergoes a period doubling sequence to chaos on a parabola, but chaos occurs for β values where the main sequence is still showing fixed point behaviour. Figures 3(e) and (f) are all for $\alpha = -0.8$ and $\beta = 3.0$ and show the spiral attractor and parabolic strange attractor which coexist with a fixed point.

The parabolic attractors develop from period doubling sequences and we have found one case where a spiral attractor arises by intermittency. It is not clear if this is generally true, as the picture is complicated in the regions of coexistence of attractors by the possibility of collisions between attractors (i.e. crises [14] of chaos) as well as more gradual transformations. It is clear that the full bifurcation diagram will be complex.

We will now examine whether the stochastic terms, which we have so far suppressed, give rise to behaviour different from that of the simple additive noise terms that have generally been studied. The behaviour of the logistic map with an additive stochastic term has indicated that at the threshold for chaos universal scaling behaviour with the strength of the noise is found. The (single) Lyapounov exponent depends on the size of the noise terms through a simple power law behaviour.

The $(\theta - z)$ map contains examples of two of the generic routes to chaos. One is the period doubling route (which of course, is also that shown by the logistic map [15]). For example, the parameter values $\alpha = -0.4$, $\beta = 2.607\,5063$ and $\lambda = 1.0$ lie near the end of the period doubling cascade and give a Lyapounov exponent of -5×10^{-5}. The three different noise terms have similar effects in that the Lyapounov exponent λ scales as

$$\lambda \propto (\varepsilon_i')^{0.38} \qquad i = 1, 2, 3 \tag{29}$$

at the onset of chaos when the ith noise term is present. This value is consistent with the value found in [16] and suggests that the effect of noise on the period doubling route to chaos is indeed governed by universal exponents even though here the noise enters the map in a completely different form from that in (28).

We have also studied an example of intermittent chaos [17] which occurs for $\alpha = 0.2$, $\beta = 1.507\,437\,93$ and $\lambda = 1.0$. In the absence of noise the exponent is -6×10^{-4}. The behaviour when noise is present is rather different from that in (29). We find that the exponents obey a scaling law of the form

$$\lambda \propto (\varepsilon_i')^{0.56} \qquad i = 1, 2 \tag{30}$$

and

$$\lambda \propto (\varepsilon_3')^{0.72} \tag{31}$$

for small noise levels. Whereas (30) is a good description of our numerical results, (31) needs to be treated with some caution. The scaling law of (30) is valid over three orders of magnitude of ε_i $(i=1,2)$ but (31) is valid only for two orders of magnitude of ε_3. Since there has been a tendency to think that any type of noise will give similar behaviour owing to the non-linearity in the deterministic evolution (and resultant mixing qualities of the flow), the different behaviour found is surprising.

The map of (25) which is rather closely related to the Lorenz model shows two routes to chaos depending on the sign of $\nu(-1-\nu')$ in the purely deterministic case. In fact, it has been argued [18] that the deterministic map represents, at least qualitatively, the dynamics of systems more general than the Lorenz model and the main requirements for a finite set of coupled non-linear multi-parameter ordinary differential equations are that

(i) there is a fixed point for which the real parts of the eigenvalues of its stability matrix can be ordered and the largest real part corresponds to a purely positive eigenvalue $\hat{\lambda}_1$ while the eigenvalue, $\hat{\lambda}_2$, with the next largest real part is a negative number,

(ii) a set of coordinates can be chosen so that the fixed point is at the origin and there is an inversion symmetry with respect to the subspace spanned by the eigenvectors associated with $\hat{\lambda}_1$ and $\hat{\lambda}_2$,

(iii) a homoclinic orbit exists.

For the Lorenz model

$$\nu = 1 - \frac{2b}{-\sigma - 1 + [(\sigma-1)^2 + 4\sigma r]^{1/2}} \tag{32}$$

and hence ν is positive. If the saddle point is such that $|\hat{\lambda}_2/\hat{\lambda}_1| > 1$, then $\nu < 0$. From standard arguments it can be shown [18] that for $\nu < 0$ there is a period doubling route [19] to chaos while for $\nu > 0$ we have a tangent bifurcation to Lorenz type chaos. If we regard the Lyapounov exponent as an order parameter, the case $\nu > 0$ corresponds to a first-order transition and the case $\nu < 0$ to a second-order one. For a first-order transition there is no scaling of λ at the transition point to chaos. At the transition λ jumps to a positive value and in the regime of fully developed chaos λ is found to be insensitive to noise (for noise strengths up to 10^{-3} and averaging over 10^6 iterations). Hence we shall concentrate on the case $\nu < 0$. It is convenient to rescale variables such that the map in (25) has the form

$$\alpha_1 \to \operatorname{sgn}(\alpha_1)(-1 + B(|\alpha_1| + \sigma_1 \xi_1|^{-\nu+1})) + \sigma_2 \xi_2 \tag{33}$$

where B, σ_1 and σ_2 are parameters. It is for certain positive B (B_C say) that we have an accumulation point for period doubling sequences. We investigate $\nu = -\frac{1}{4}, -\frac{1}{2}$ and -1. The respective B_C are $B_C = 1.209\,513,\ 1.295\,509,\ 1.401\,155$. At B_C

$$\lambda \propto (\sigma_i)^{0.326} \qquad \text{for } \nu = -\tfrac{1}{4} \tag{34}$$

$$\propto (\sigma_i)^{0.357} \qquad \text{for } \nu = -\tfrac{1}{2} \tag{35}$$

$$\propto (\sigma_i)^{0.37} \qquad \text{for } \nu = -1. \tag{36}$$

Equation (36) is consistent with (29) and the standard logistic map result. As noted by Arneodo *et al* [5] in the deterministic case the continuous map associated with (33) (by removing the factor $\operatorname{sgn}(\alpha_1)$) has the same derivative (up to a sign) as the

discontinuous map whose derivative is positive and this holds also for the higher-order derivatives. This leads to close correspondences in the bifurcation structures. For $\nu = -1$ the logistic map is the associated continuous map. From the theory of continuous maps [19] it is known that one of the factors determining the universality class of the maps is the behaviour near the origin. Hence it is not surprising that (34)-(36) show that the scaling of the Lyapounov exponent changes with ν.

These examples of stochastic Shilnikov maps have been shown to exhibit a rich variety of behaviour. They represent arguably a more natural introduction of noise into maps for dynamical systems. They show period doubling routes to chaos, intermittency, coexistent attractors, second- and first-order transitions to chaos, hysteresis effects and so on. It is possible that they will be helpful in obtaining a deeper understanding of quantum chaos in dissipative systems [20], equations for which can often be represented in a form similar to that of (1) and (20) in a space of suitable dimensionality.

Acknowledgments

One of us (SS) would like to thank D S Broomhead for helpful discussions. JSS wishes to thank RSRE, Malvern, for the funding of his Research Assistantship at the Clarendon Laboratory, University of Oxford.

References

[1] Lichtenberg A J and Lieberman M A 1983 *Regular and Stochastic Motion* (Berlin: Springer)
[2] Guckenheimer J and Holmes P 1983 *Non-linear Oscillations, Dynamical Systems and Bifurcations of Vector Fields* (Berlin: Springer)
[3] Smale S 1980 *The Mathematics of Time* (Berlin: Springer)
[4] Shilnikov L P 1970 *Math. USSR Sb.* **10** 91
[5] Arneodo A, Coullet P and Tresser C 1981 *Phys. Lett.* **81A** 197
Sparrow C 1982 *The Lorenz Equations: Bifurcations, Chaos, and Strange Attractors* (Berlin: Springer)
Fowler A 1986 *Nonlinear Phenomena and Chaos* ed S Sarkar (Bristol: Adam Hilger) p 284
[6] Zippelius A and Lücke M 1981 *J. Stat. Phys.* **24** 345
[7] Sarkar S, Satchell J S and Carmichael H J 1986 *J. Phys. A: Math. Gen.* **19** 2751
[8] Callen H B and Welton T A 1951 *Phys. Rev.* **83** 34
Nyquist H 1928 *Phys. Rev.* **32** 110
[9] Crutchfield J P and Packard N H 1983 *Physica* **7D** 201
Haken H and Mayer-Kress G 1981 *J. Stat. Phys.* **26** 149
Shraiman B, Wayne C E and Martin P C 1981 *Phys. Rev. Lett.* **46** 935
Feigenbaum M and Hasslacher B 1982 *Phys. Rev. Lett.* **49** 605
[10] Eckmann J-P and Ruelle D 1985 *Rev. Mod. Phys.* **57** 617
Farmer J D 1982 *Z. Naturf.* **37a** 1304
[11] Termonia Y and Alexandrowicz Z 1983 *Phys. Rev. Lett.* **51** 1265
Mandelbrot B B 1982 *The Fractal Geometry of Nature* (San Francisco: Freeman)
[12] Gardiner C W 1983 *Handbook of Stochastic Methods* (Berlin: Springer)
Uhlenbeck G E and Ornstein L S 1930 *Phys. Rev.* **36** 823
[13] Lorenz E N 1963 *J. Atmos. Sci.* **20** 130
[14] Grebogi C, Ott E and Yorke J A 1983 *Physica* **7D** 181
[15] Feigenbaum M J 1978 *J. Stat. Phys.* **19** 25
[16] Crutchfield J, Nauenberg M and Rudnick J 1981 *Phys. Rev. Lett.* **46** 933
[17] Pomeau Y and Manneville P 1980 *Commun. Math. Phys.* **74** 189
Hirsch J E, Nauenberg M and Scalapino D J 1982 *Phys. Lett.* **87A** 391

Eckmann J P, Thomas L and Wittwer P 1981 *J. Phys. A: Math. Gen.* **14** 3153
[18] Lyubimov D V and Zaks M A 1983 *Physica* **9D** 52
[19] Feigenbaum M J 1979 *J. Stat. Phys.* **21** 669
[20] Sarkar S and Satchell J S 1987 *Phys. Rev.* A to be published